Paleoceanography and Paleoclimatology

RESEARCH ARTICLE
10.1029/2021PA004249

Key Points:

- Analysis of the distribution of area density values provides a method for assessing sample preservation
- Area density values can be used to assess influences related to cryptic speciation and shell preservation
- Well-preserved thin and very thin shells retain a surface ocean signature correlating with surface ocean carbonate ion concentrations

Supporting Information:

Supporting Information may be found in the online version of this article.

Correspondence to:

N. E. Umling,
numling@amnh.org

Citation:

Umling, N. E., Saad, B., Sikes, E., & Goodkin, N. F. (2021). Proximity to undersaturation and the influences on *G. bulloides* area-density in southern Indian Ocean marine sediments. *Paleoceanography and Paleoclimatology*, *36*, e2021PA004249. https://doi.org/10.1029/2021PA004249

Received 4 MAR 2021
Accepted 13 MAY 2021

Proximity to Undersaturation and the Influences on *G. bulloides* Area-Density in Southern Indian Ocean Marine Sediments

N. E. Umling[1], B. Saad[1,2], E. Sikes[3], and N. F. Goodkin[1]

[1]Department of Earth and Planetary Sciences, American Museum of Natural History, New York, NY, USA, [2]Department of Environmental Sciences, Barnard College, New York, NY, USA, [3]Department of Marine and Coastal Sciences, Rutgers University, New Brunswick, NJ, USA

Abstract The area density proxy of foraminiferal shell thickness and calcification intensity has the potential to provide information about past ocean CO_2 content and has the benefit of small sample requirements, simple analytical techniques, and the ability to re-use the analyzed foraminifera for other paleo-proxies. Using a series of multicore core-tops collected from the southeastern Indian Ocean (1.8–3.8 km water depth), we evaluate the reliability of utilizing area density values of *Globigerina bulloides* from sediment cores to estimate surface ocean carbonate parameters. Because foraminifera in marine sediments can rarely be considered "pristine" (or "glassy"), we grouped area density measurements of shells to designate various stages of diagenesis. Visual signs of alteration were apparent at area density values as low as $\sim 0.122 \times 10^4$ μg/μm^2, with deviations from the "pristine" endmember beginning at area density values of $\sim 0.087 \times 10^4$ μg/μm^2. We find that increases in area density overprint the surface ocean carbonate signature in thicker ($>0.122 \times 10^4$ μg/μm^2 shells), but small increases associated with marine sedimentary burial and diagenesis can be accounted for, allowing this proxy to be applied back in time. Reconstructing the distribution of area density values in a given sample has the potential to provide valuable information on overall sample preservation by estimating the percent of well-preserved shells ($<0.122 \times 10^4$ μg/μm^2; %wp) in a given sample. Our %wp metric has the potential for use as a proxy for lysocline variability in addition to assessing the suitability of marine sediment samples for surface ocean reconstructions.

1. Introduction

The formation and dissolution of biogenic calcium carbonate ($CaCO_3$) plays an important role in the natural pH buffering capacity of the world's oceans. When forming $CaCO_3$ shells (tests), planktic foraminifera sequester atmospheric CO_2 by transferring both alkalinity and dissolved inorganic carbon (DIC) from the surface to the deep ocean, where it can remain for thousands of years. Primary production constitutes the other contribution of the biological pump to the carbon buffering system. In situ respiration in the deep ocean increases CO_2 content and subsequently increases the acidity of the deep ocean. This initiates a feedback mechanism in which dissolution of $CaCO_3$ shells on the seafloor releases alkalinity and buffers a portion of the additional CO_2. Since industrialization, oceanic uptake of anthropogenic CO_2 has resulted in a 26% increase in the acidity of surface ocean waters (IPCC, 2014) increasing our imperative to understand changes to the interactions of ocean CO_2 content and the components of the biological pump. Understanding and predicting the impacts of present and future ocean acidification requires a better understanding of past ocean-atmosphere CO_2 exchange which can be achieved through reconstructions of past surface carbonate saturation and pCO_2.

Morphometric proxies of shell thickness and calcification intensity have the potential as an analytically simple proxy for reconstructing surface ocean carbonate saturation, with the benefit of small sample requirements and the ability to re-use the analyzed foraminifera for geochemical analyses. Morphometric-based proxies exploit the link between surface ocean carbonate chemistry and rates of planktic foraminifera calcification that has been observed in plankton tows, sediment trap samples (Beer et al., 2010; Moy et al., 2009; Osborne et al., 2016; Weinkauf et al., 2016) and culture experiments (Davis et al., 2017). Nonetheless, there remains some uncertainty as to whether this signal is preserved in fossil planktic foraminifera shells in

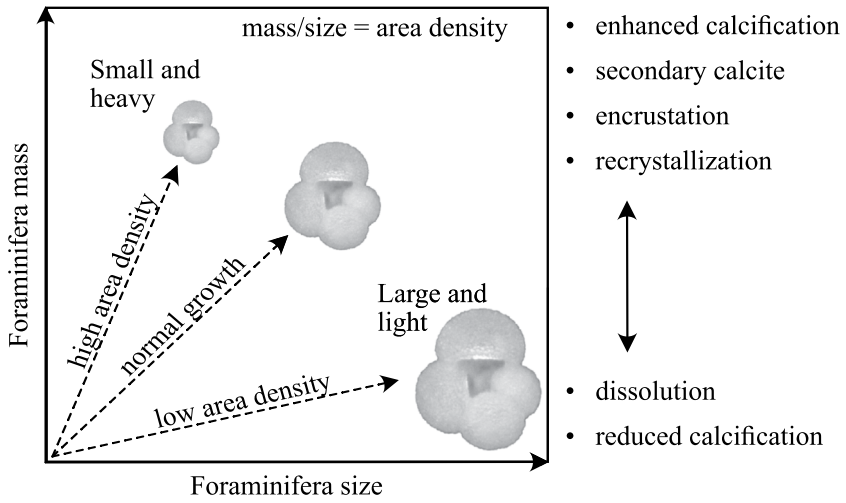

Figure 1. As foraminifera grow, they add chambers and increase in both size and mass. Processes like enhanced calcification, recrystallization, encrustation, and the formation of secondary calcite can increase shell mass while dissolution and decreased calcification can decrease shell mass, both with small to negligible changes to shell size. Area density can normalize shell mass for size without confining shells to a narrow size range. A shell lighter than expected for a given size will have a low area density value. Likewise, a shell heavier than expected for a given size will have a high area density value.

sediment cores because of concerns about processes such as calcite dissolution and the formation of authigenic crusts overprint the primary surface ocean signature with a secondary deep-ocean signature (Broecker & Clark, 2001; Qin et al., 2017).

As foraminifera grow, they add calcite and increase mass (Figure 1). Calcification rates during the life of the foraminifera have been shown to be influenced by surface ocean carbonate saturation with thinner, lighter shells found in waters undersaturated in carbonate ion (Barker & Elderfield, 2002; Bijma et al., 2002; de Moel et al., 2009; Marshall et al., 2013; Moy et al., 2009; Osborne et al., 2016, 2020; Weinkauf et al., 2016). After a planktic foraminifera dies, shell mass and chemistry can be altered by a variety of diagenetic processes such as (a) dissolution of original calcite (Bé et al., 1975; Berger, 1970; Brown & Elderfield, 1996), (b) pore fluid precipitation of geochemically distinct material as an encrustation or overgrowth on interior or exterior of shells walls (Branson et al., 2015; Detlef et al., 2020; Edgar et al., 2015; Metcalfe, 2013; Millo et al., 2005; Pena et al., 2005; Reimers et al., 1996; Sexton et al., 2006; Wycech et al., 2016), and (c) recrystallization (or neomorphism) of the original shell wall with new calcite formed in-situ (Edgar et al., 2015; Gibson et al., 2016; Lorens et al., 1977; Pearson & Burgess, 2008). These processes can increase or decrease shell mass. Partial dissolution of shell calcite bathed in waters undersaturated with respect to carbonate ion can decrease shell mass while having only a minor effect on shell size, up to the point that dissolution is extensive enough to result in the shell fragmentating and breaking into pieces (Bé et al., 1975; Berger, 1970; Brown & Elderfield, 1996; Lohmann, 1995; Savin & Douglas, 1973). Conversely, partial dissolution with subsequent recrystallization and/or crust formation can result in an increase in shell mass due to replacement of dissolved calcite with new additional calcite formed in-situ (Pearson et al., 2001; Schiebel et al., 2007; Sexton et al., 2006). Because recrystallization of biogenic calcite can occur at the nanoscale, new calcite may be nearly indistinguishable from the original shell material (Sexton et al., 2006).

The relationship between size and mass that has been established for "pristine" foraminifera collected in sediment traps can be compared with sedimentary foraminiferal shells to monitor changes in the relationship between size and mass that can be associated with dissolution, encrustation, or recrystallization of shell calcite. We expect an encrusted or recrystallized shell to be thicker and heavier than expected for a pristine shell of similar size. Likewise, a shell that has experienced only dissolution should be thinner and lighter than expected for a pristine shell of similar size. Here, we utilize the area density proxy (ρ_A; Marshall et al., 2013) of foraminiferal calcification to evaluate shell thicknesses and masses in a suite of sediment cores collected from the southern Indian Ocean. The area density calculation investigates size-independent

Table 1
Locations and Depths of Southeastern Indian Ocean Multicores (MC) Utilized in This Study

Location	Core name	Latitude (°S)	Longitude (°E)	Depth (m)
Southeast Indian Ridge	**TT1811-31MC**	−42.481	80.590	2,981
Southeast Indian Ridge	**TT1811-32MC**	−41.717	80.161	3,174
Southeast Indian Ridge	**TT1811-36MC**	−40.745	79.928	3,035
Southeast Indian Ridge	**TT1811-38MC**	−40.156	79.055	2,845
Île Amsterdam	**TT1811-40MC**	−39.663	78.775	2,954
Île Amsterdam	**TT1811-43MC**	−38.150	79.105	1,796
Île Amsterdam	**TT1811-45MC**	−38.475	78.745	2,034
Île Amsterdam	**TT1811-60MC**	−38.301	77.424	1,930
Île Amsterdam	**TT1811-65MC**	−38.339	77.129	2,568
90°E ridge	**TT1811-74MC**	−34.011	82.352	3,512
90°E ridge	**TT1811-77MC**	−32.260	85.942	3,825

calcification influences while retaining information on the individual variability within a population. We also evaluate the influence of diagenesis on *G. bulloides* area density values with the aim of understanding the utility and limits of the area density carbonate ion paleo-proxy.

2. Materials and Methods

2.1. Sites and Samples

We utilize a series of multi-cores (MCs) collected by the Research Vessel Thomas G. Thompson in late-2018 (TT1811) during the Coring to Reconstruct Oxygen and Carbon Dioxide Across 2 Seas (CROCCA-2S) cruise to the Southern Indian Ocean. The TT1811 MCs span water depths from 1,796 to 3,825 m, latitudes from 32.260 to 42.481°S, and longitudes from 77.129 to 85.942°E (Table 1), capturing the southeastern quadrant of the Indian Ocean (Figure 2). The range of core depths allows us to investigate the influence of progressive diagenesis on foraminifera shell weight and thickness records as deep-water carbonate ion saturation decreases.

We measured area density values for *Globigerina bulloides*, a planktic foraminifera species abundant in subpolar and transitional zones, low latitude upwelling systems, and subtropical zones (Bé, 1977; Bé & Tolderlund, 1971; Darling et al., 2000; Kretschmer et al., 2018; Peeters & Brummer, 2002; Sautter & Thunell, 1991). As *G. bulloides* does not form symbiotic relationships with photosynthetic algae, its distribution is partially driven by food availability (Field, 2004; Iwasaki et al., 2017; Kretschmer et al., 2018; Kuroyanagi & Kawahata, 2004; Mortyn & Charles, 2003; Ortiz et al., 1995; Peeters & Brummer, 2002; Wilke et al., 2009) and varies seasonally with changes in upwelling and shifts in the deep chlorophyll maximum (Kretschmer et al., 2018;

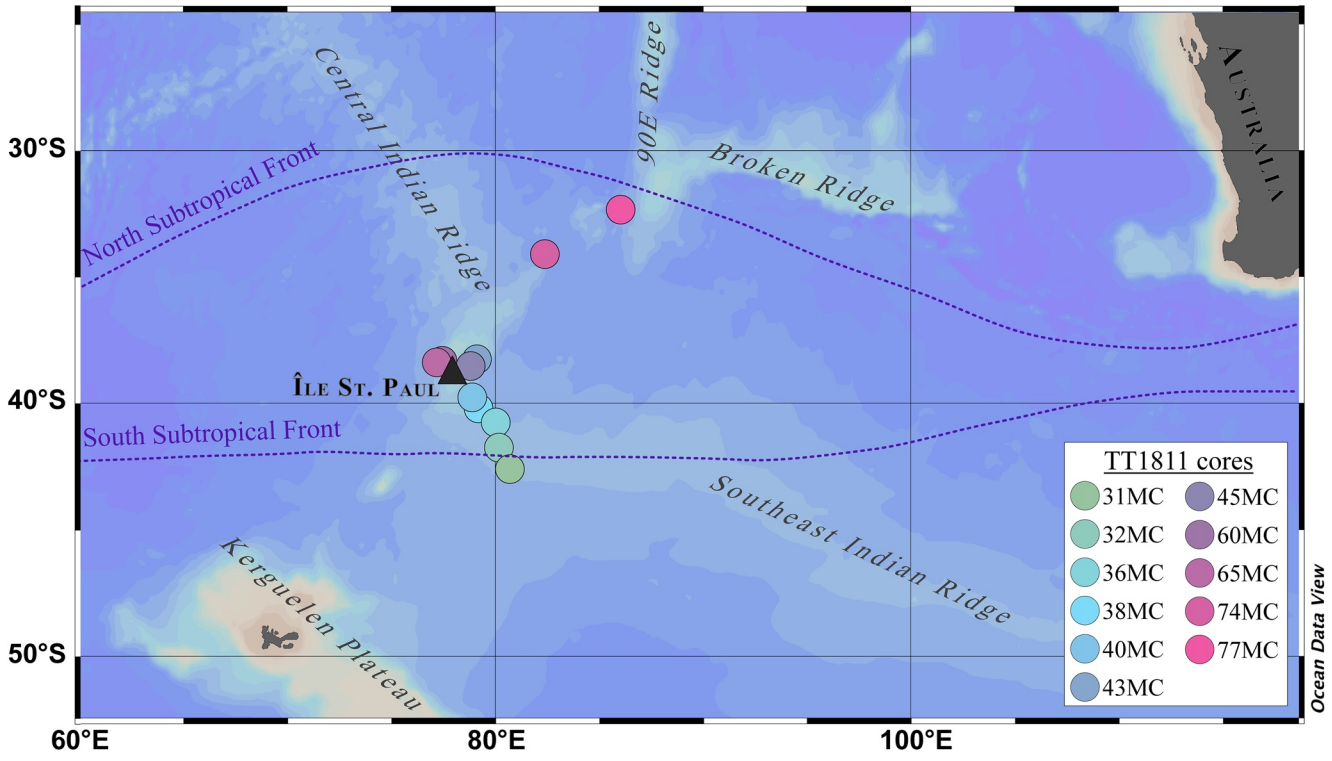

Figure 2. Location and regional hydrography of the multicores used in this study. Regional bathymetric features are labeled, and frontal boundaries are indicated by dashed lines. The location of volcanic island Île St. Paul is indicated by a triangle.

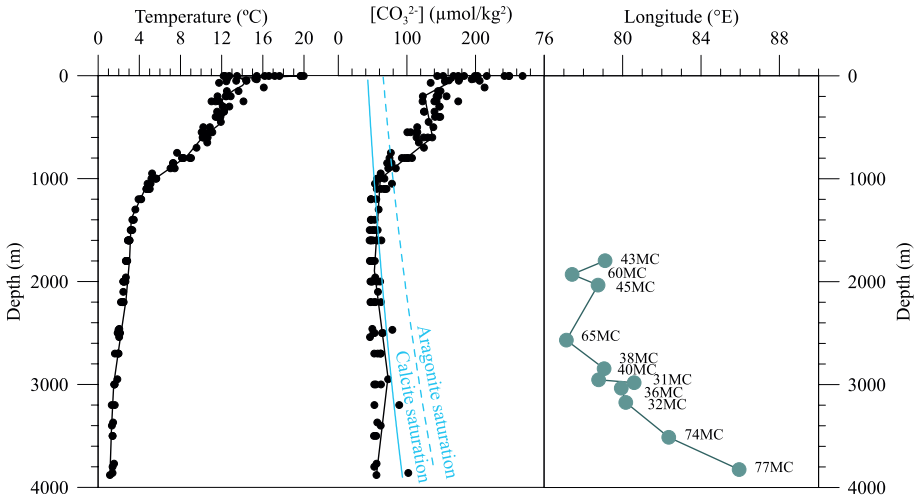

Figure 3. Temperature and phosphate were measured from bottle data and carbonate ion was estimated from pH and dissolved inorganic carbon measurements. The utilized multicores were bathed in waters close to or below calcite saturation, with the two deepest cores (74 and 77 MC) collected from the most undersaturated waters recorded in this study.

Reynolds & Thunell, 1985; Sautter and Thunell, 1989, 1991; Thunell & Reynolds, 1984) which ranges from ~0 to100 m across our study region (Figure 3).

The asymbiotic species *G. bulloides* deposits minor amounts of secondary calcite (Schiebel et al., 1997; Spero & Lea, 1996) during reproduction (gametogenesis) when many planktic foraminifera species deposit an additional chamber (i.e., the final sac-like chamber of *Trilobatus sacculifer*) or a final layer of thickened calcite (gametogenic calcite; Hemleben et al., 1989) prior to gamete release. In some species, gametogenic calcite comprises a large percentage of total shell calcite (~28% for *T. sacculifer* and >80% for *Orbulina universa*; Bé, 1980; Hamilton et al., 2008). Consequently, a population of foraminifera that includes individuals that have both completed and not completed gametogenesis could obscure the relationship between shell weight proxies and carbonate chemistry. Accordingly, our choice of size fraction is based on plankton tow data suggesting that close to 100% of *G. bulloides* larger than ~150 µm have completed gametogenesis (Schiebel et al., 1997).

2.2. Hydrographic Measurements

Seawater samples were collected from multiple depths at each CROCCA-2S water sampling station using a SeaBird CTD with a Nisken bottle Rosette. Total phosphate was measured in the Rutgers Nutrient Analysis Laboratory. Seawater pH was measured at sea using a HACH multimeter in 50 mL subsamples within 1 h of collection. The multimeter was calibrated each day with a three-point calibration curve (pH_{NBS} = 4, 7, 10). Seawater DIC was measured at the University of Florida using a UIC (Coulometrics) 5017 CO_2 coulometer coupled with an AutoMate automated carbonate preparation device (AutoMateFX.com). Five mL of sample was weighed into septum top tubes and placed into the AutoMate carousel. 10% Phosphoric acid and CO_2-free nitrogen carrier gas was then injected into the sample vial through a double needle assembly and evolved CO_2 was carried through a silver nitrate scrubber to the coulometer where total C was measured.

Seawater carbon speciation was calculated from pH_{NBS} and DIC using the seacarb package (Lavigne et al., 2011) in R. The K_1 and K_2 constants from Lueker et al. (2000) were used except for samples with temperatures below 2°C, in which case the K_1 and K_2 constants from Waters et al. (2014) were used. The K_f from Perez and Fraga (1987) was used for samples with temperatures above 9°C and the K_f from Dickson and Riley (1979) was used for samples with temperatures below 9°C. The K_s from Dickson (1990) was used for all samples.

2.3. Area Density and Area Normalized Shell Weights

To obtain information about intra-sample variability, we estimated individual *G. bulloides* area density values (ρ_A; Marshall et al., 2013), where A refers to silhouette area, A_{if} refers to individual foraminifera silhouette area, and M_{if} refers to individual foraminifera mass (Equation 1). Individual area density values were then averaged for each MC core top sample.

$$\rho A = M_{if} \ / \ A_{if} \quad (1)$$

G. bulloides shells (n = 39–64 per sample) were selected from the >250 μm size fraction and photographed umbilical side up using a binocular microscope fitted with an AmScope MU1000 camera with a 1.67 × 1.67 μm pixel resolution. Imaged shell silhouette areas and Ferret diameters were analyzed using the open-source image processing program ImageJ with the processing package Fiji (Schindelin et al., 2012). Images were calibrated using a 1 mm micro-scale photographed at the same magnification as the foraminifera shells. Individual foraminifera were weighed using a Mettler Toledo XPR2 analytical balance (±0.8 μg). The reproducibility and error of the balance was monitored through repeat measurements (5–10x) of individual foraminifera throughout each weighing session, re-zeroing between each measurement and previously measured sample masses were spot-checked to confirm masses were reproducible from day-to-day ensuring balance reproducibility was consistent across the range of foraminifera masses included in this study (Figure S1). Samples were not treated chemically as several studies have noted negligible impacts of pre-treatment on shell weights aside from both positive and negative deviations in mass associated with the inclusion of a sodium hexametaphosphate (Calgon®) soak (Marshall et al., 2013; Metcalfe, 2013).

After individual foraminifera were photographed and weighed, ~2–5 *G. bulloides* were selected from each core top sample for Scanning Electron Microscope (SEM) imaging to assess shell preservation through examination of shell ultrastructure at 700–1,300xmagnification on a Zeiss EVO 60 variable pressure SEM at the American Museum of Natural History. In preparation for SEM imaging, *G. bulloides* were gently broken to expose cross sections through the ultimate and penultimate shell chamber walls, mounted on carbon tape, and gold sputter-coated.

Dissolution was assessed following Dittert and Henrich (2000) through examination of shell ultrastructure at. *G. bulloides* were considered very well-preserved if they had distinct spine bases, ridges, and pores with no signs of etching to the interpore area or shell wall (Figure S2). Moderately well-preserved *G. bulloides* showed only minor erosion to spine bases, ridges, and pores with some minor signs of etching to the interpore area. *G. bulloides* were considered poorly preserved when signs of moderate to major erosion of spine bases, ridges, and pores were observed, or there were signs of hair-cracks and/or peeled calcite layers. Additionally, *G. bulloides* were assessed for more advanced stages of dissolution in which shells were monitored for cracks and holes in the shell wall, interconnected pores, completely eroded spine bases and ridges, and/or missing calcite layers. Stained or broken shells were excluded from our analyses.

3. Results

Dissolution indices from core top-studies suggest that the lysocline in the eastern tropical Indian Ocean is located close to 3,800 m water depth (Peterson & Prell, 1985), but dissolution is suspected to occur shallower in the water column (Regenberg et al., 2014; Schiebel et al., 2007). Estimates of deep ocean carbonate ion concentration ($[CO_3^{2-}]$) suggest saturation values that lie close to and slightly below calcite saturation over an extended depth range spanning nearly 2,000 m (From ~1,200 to 3,000 m) in the Southeastern Indian Ocean (Figure 3). All of the multicores included in this study were collected from depths close to or below carbonate saturation with only the two deepest cores within undersaturated bottom waters (74 and 77 MC).

The 767 individual *G. bulloides* weighed and photographed from the TT1811 multicores ranged in mass from ~1.9 to 72 μg ($\overline{x}$ = 11.2 ± 5.9 ug) with Feret diameters (longest axis) ranging from ~300 to 625 μm ($\overline{x}$ = 380.7 μm; Figure 4). Relative to published area density values from the Santa Barbara Basin (SBB; Osborne et al., 2016) sediment trap time series, core-top *G. bulloides* shells are generally heavier than expected for a given area (Figure 4a). Shell silhouette area and diameter are highly correlated, indicating that both metrics should be effective for normalizing weights (Figure 4b). Excluding outliers (ρ_A > 0.205 μg/μm^2),

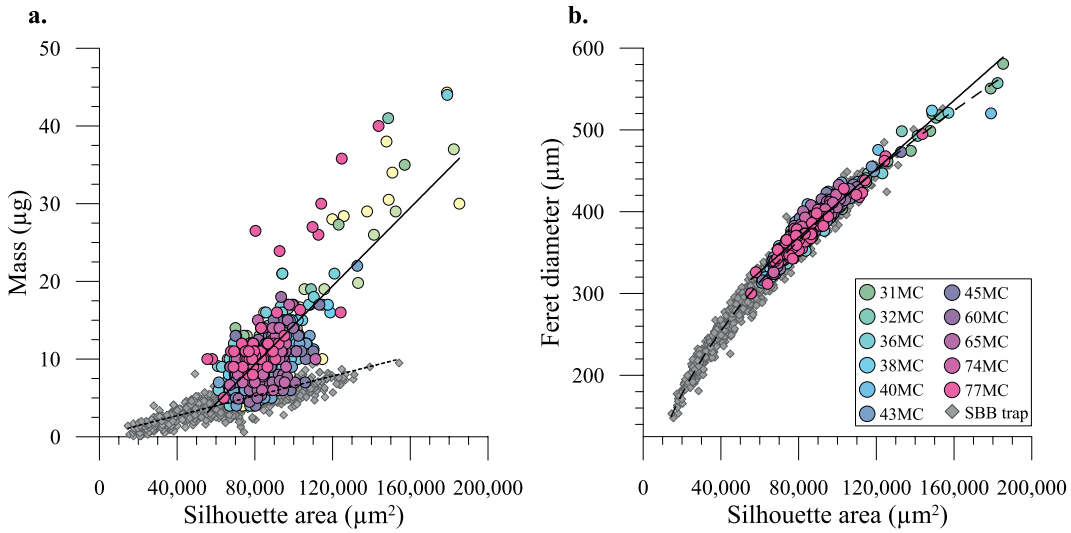

Figure 4. Individual shell mass, silhouette area, and Feret diameter measurements describing the morphometric characteristics of *G. bulloides* in the southern Indian Ocean multicore core tops and the Santa Barbara Basin (SBB) sediment trap time series. (a) Southern Indian Ocean mass and silhouette area are moderately well correlated ($R^2 = 0.63$; solid line) with generally heavier shells than predicted by the SBB sediment trap mass-area relationship ($R^2 = 0.65$; dotted line). (b) Southern Indian Ocean *G. bulloides* silhouette areas and Feret diameter are well correlated ($R^2 = 0.93$), with increased Feret diameter variability among shells with larger silhouette areas (>160,000 µm^2). The mass-area relationship for both core-top and sediment trap *G. bulloides* shows a power distribution ($R^2 = 0.98$) with smaller changes in silhouette area for shells with small diameters relative to larger diameter shells.

the multicore area density values were normally distributed (Shapiro-Wilk test, W = 0.09951, p = 0.06427; Figure 5).

Individual *G. bulloides* were classified into four thickness categories according to measured area density values (Figure 5); very thick (>0.160 × 10^4 µg/µm^2), thick (0.122 × 10^4–0.160 × 10^4 µg/µm^2), thin (0.087 × 10^4–0.122 × 10^4 µg/µm^2), and very thin (<0.087 × 10^4 µg/µm^2). SEM examination of outlier specimens often included crystalline surface textures or signs of moderate to high levels of post-depositional dissolution, such as pitted and coarse wall texture, eroded spine bases and ridges, formation of cracks, and even peeled calcite layers as described using the metrics of Dittert and Henrich (2000). Evidence of moderate to high dissolution was observed in *G. bulloides* with area density values as low as 0.122 × 10^4 µg/µm^2, with both thick and very thick shells observed at various stages of dissolution (Figure 6). SEM imaged thin and very thin shells were well preserved with evidence of only minor erosion to spine bases, ridges, and pores (Figure 6). Under reflected light, the thick and very thick shells were generally opaque ("frosty") in appearance, whereas the thin and very thin shells were fully or partially translucent ("glassy").

Published area density values from the SBB (Osborne et al., 2016) sediment trap time series were used to define the boundary between very thin and thin shells in this study. The SBB time series represents a population of pristine individuals from a region dominated by a single *G. bulloides* genotype (type IId) with minor influences from a secondary, more thickly calcified *G. bulloides* genotype (type IIa) during upwelling periods (Darling et al., 2003). At present, genetic studies have identified 18 distinct genotypes within the *G. bulloides* morphospecies (Darling et al., 2017). These species fall within two distinct groups of genotypes showing ecologically driven distributions, with four warm water cluster genotypes (Type I) found in subtropical and tropical zones and seven cool water cluster genotypes found in cooler subpolar and transitional zones (Type II; Darling & Wade, 2008; Darling et al., 2017). Two of the *G. bulloides* genotypes have been identified in the Arabian Sea (IIf + Ia; Darling et al., 2017; Sadekov et al., 2016) and four have been identified in the southern Indian Ocean (IIb, IIa, IIc, IIg; Morard et al., 2013). Our warmer core sites are likely dominated by Type IIb, however Type IIa may become more prevalent at the cooler, more southerly sites with small amounts of Type IIc present at the most southerly sites (Morard et al., 2013).

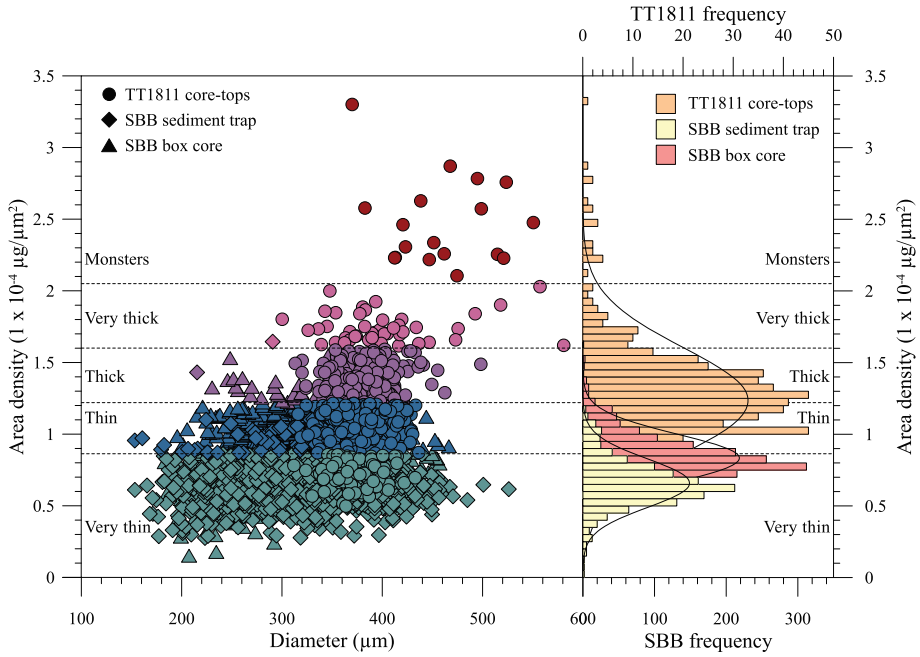

Figure 5. Indian Ocean core top samples document a large range of area density values across a narrow range of diameters. A histogram showing the frequency of individual *G. bulloides* area density values for 0.05×10^4 µg/µm^2 bins indicates that Indian Ocean core top individuals were primarily classified as thin or thick. In contrast, Santa Barbara Basin (SBB) box core (Osborne et al., 2020) and sediment trap samples (Osborne et al., 2016) document a narrow range of area density values primarily classified as very thin, with a shift toward slightly higher area density values in the SBB box core samples. The sediment trap data defines a "pristine" endmember, thus the 90th percentile of the sediment trap distribution was used to define the boundary between thin and very thin shells. The tail of the sediment trap distribution corresponds to the 50th percentile of the multicore core-top data which defines the boundary between thin and thick shells. The 90th percentile of the multicore core-top data defines the boundary between thick and very thick shells. The large "monster" shells comprise a long tail in the distribution of the core-top data and are statistical outliers. Dashed lines indicate maximum and/or minimum area density values used for shell thickness classifications.

The 90th percentile value of area density estimated from the SBB time series (0.087×10^4 µg/µm^2) was used to define the boundary between very thin and thin *G. bulloides*. Although the dominant *G. bulloides* genotype in SBB (type IId) has only been identified in the northeast Pacific and is not expected in the Indian Ocean (Morard et al., 2013; Sadekov et al., 2016), several of our Indian Ocean multicore core-tops show a bimodal or multimodal distribution with one peak centered at the mean area density value recorded by the SBB sediment trap *G. bulloides* ($\bar{x} = 0.066 \times 10^4$ µg/µm^2; Figure 7). This was particularly evident in 65 and 36 MC (Figure 7), for which bootstrap resampling suggests a robust bimodal distribution (Figure S3). The sediment trap samples provide a pristine endmember with which we can anchor the core-top values and because there is a limit to how thin shells can be, the sediment trap anchor should be robust through time. The multicore core-tops with multimodal distributions show peaks roughly divided at the mean value of the TT1811 data (0.122×10^4 µg/µm^2; Figures 5 and 7) and close to the upper limit of the sediment trap

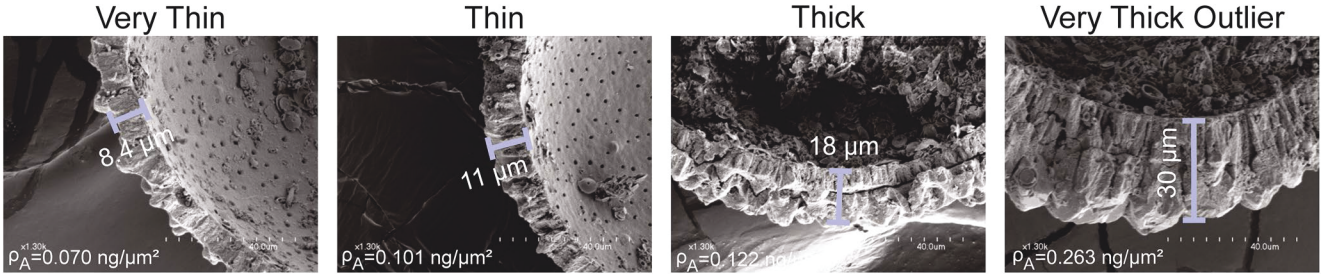

Figure 6. Scanning Electron Microscope imaging of *G. bulloides* individuals representing the spread of area density values.

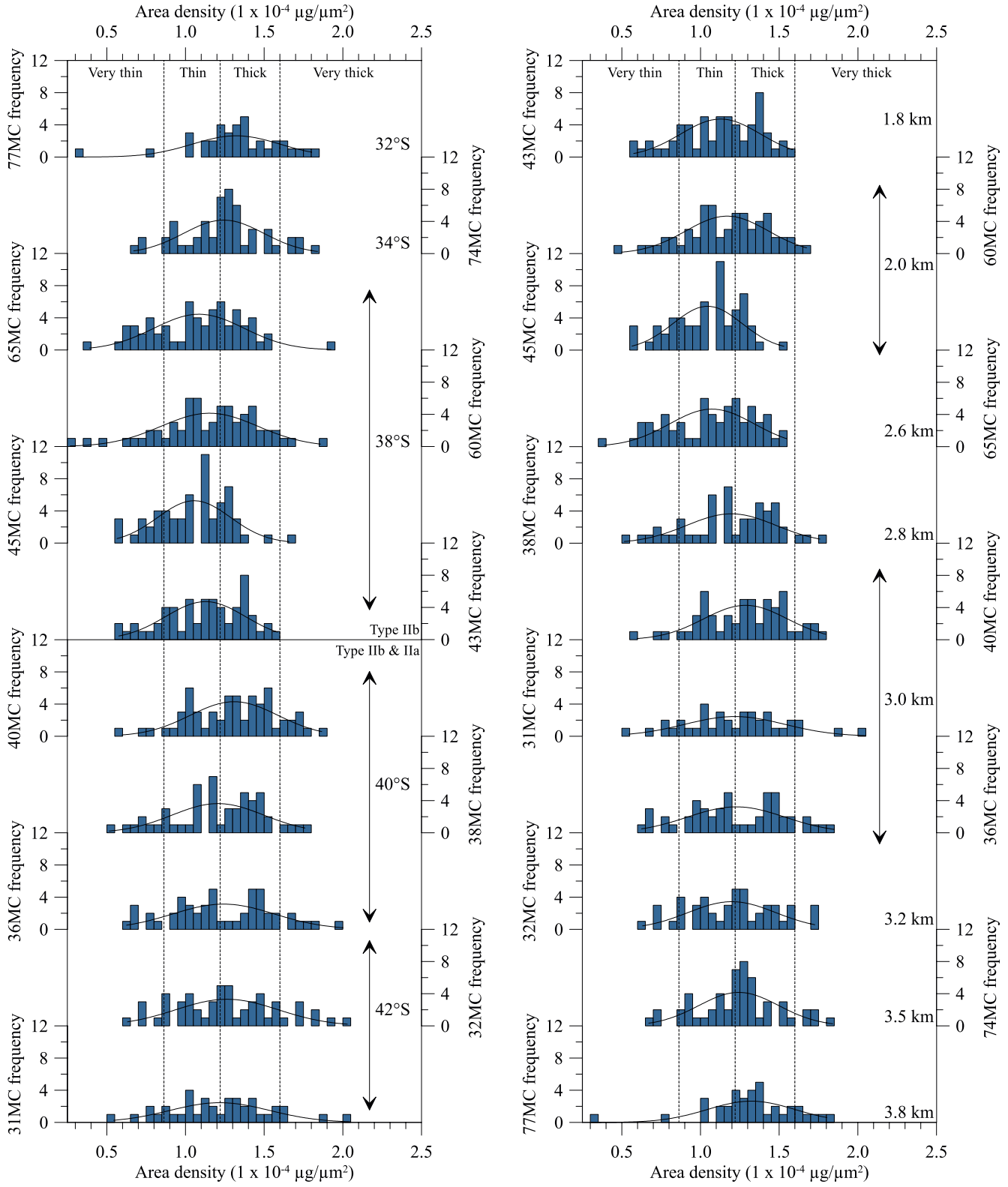

Figure 7. Histograms for each multicore core-top show the frequency of *G. bulloides* area density values across 0.05×10^4 µg/µm^2 bins. (a) Individual core-top frequency distributions do not show a consistent pattern with increasing latitude. (b) Individual core-top frequency distributions show a shift toward larger area density values with increasing core depth. The deepest cores (32, 74, and 77 MC) have few shells classified as very thin and more shells classified as thick or very thick relative to the shallowest cores (43, 60, 45, 65 MC) which have few very thick shells and more thin or very thin shells.

distribution. Consequently, the value 0.122×10^4 μg/μm^2 was used to define the division between thin and thick *G. bulloides*. Similar to the SBB time series, the 90th percentile value estimated for the TT1811 cores was used to define the boundary between very thick and thick *G. bulloides*. The largest shells ("monsters"; $>0.205 \times 10^4$ μg/μm^2) comprise a long tail in the distribution of core top data and are statistical outliers.

Simple linear regressions of area density with surface ocean (CO_3^{2-}) in our multicores indicate that average area density values for thick, thin, and very thin shells are significant to moderately well correlated with surface ocean (CO_3^{2-}) (Table S1). Thin and very thin shells are positively correlated with surface ocean (CO_3^{2-}), but, in contrast to both thin and very thin shells along with the results from the SBB sediment trap (Osborne et al., 2016), thick shells are negatively correlated with surface ocean (CO_3^{2-}). Simple linear regressions of thick, thin, and very thin average area density values with deep ocean (CO_3^{2-}) are not significant (Table S2), suggesting that the foraminifera area density values are not documenting deep water properties.

4. Disentangling Influences on Core-Top Area Density Variability

An increase in *G. bulloides* area density values could be associated with either an increase in surface water carbonate saturation (Davis et al., 2017; Osborne et al., 2016; Weinkauf et al., 2016), a more heavily calcifying cryptic species (Osborne et al., 2016), or sedimentary diagenetic processes such as recrystallization (Edgar et al., 2015; Lorens et al., 1977; Pearson & Burgess, 2008) and/or the formation of encrustations or overgrowths (Branson et al., 2015; Edgar et al., 2015; Metcalfe, 2013; Millo et al., 2005; Pena et al., 2005; Sexton et al., 2006; Wycech et al., 2016). Genetically distinct, phenotypically similar, cryptic planktic foraminifera species have been suggested to have different calcification rates and depth habitats leading to different area density values (Marshall et al., 2015; Osborne et al., 2016). Diagenetically driven shifts to the relationship between mass and size after the foraminifera has died (Lohmann, 1995) can also overprint the relationship between calcification and surface ocean conditions. The influence of cryptic speciation and diagenesis add a complicating factor to interpreting area density values. These opposing controls vary spatially in the Indian ocean and can be used to determine their relative influence. Genetic analyses on Southern Indian Ocean *G. bulloides* collected in plankton tows demonstrate increased genetic diversity with increasing latitude and decreasing SST (Morard et al., 2013). In contrast, diagenetic influences, like dissolution and authigenic crust formation, increase with depth. If *G. bulloides* area density values are primarily influenced by genetic diversity and cryptic speciation, then we would expect shifts in core-top area density values to correlate with latitude. If *G. bulloides* area density values are primarily influenced by diagenetic processes, then we would expect correlation with core water depth rather than latitude.

The distribution of individual *G. bulloides* area density values were assessed with increasing latitude (Figure 7a) and with increasing water depth for each core site (Figure 7b). The distribution of *G. bulloides* shows neither a progressive shift with latitude nor a stepped shift associated with variation in water mass frontal boundaries or cryptic species distributions recorded in the Southern Indian Ocean plankton tows (Morard et al., 2013, Figure 7a). In contrast, there is a progressive shift in *G. bulloides* distribution with water depth (Figure 7b). As water depth increases, core-tops contain fewer very thin *G. bulloides* and more very thick *G. bulloides*. Very thin *G. bulloides* should be most susceptible to dissolution and no longer be preserved as whole shells in the deeper cores collected from more undersaturated waters, consistent with the shift in very thin shells distribution we observe in the Indian Ocean core tops (Figure 7b). While our SEM images suggest that very thick *G. bulloides* are indeed impacted by dissolution as defined by the metrics of Dittert and Henrich (2000; Figure 6), it is also likely that the thicker shells are more resilient and resistant to fragmentation. However, the core-specific *G. bulloides* distributions suggest that there is not just a loss of very thin shells in deeper cores, but the addition of very thick shells not observed as frequently in shallower cores (Figure 7b). This suggests that thicker *G. bulloides* are both more resistant to fragmentation and are also precipitating authigenic crusts or experiencing recrystallization, resulting in heavier shells and higher area density values than in the shallower core tops (Figure 7b).

Another metric that has been qualitatively used to assess foraminiferal preservation is the relative transparency of the shell when viewed under reflected light (Sexton et al., 2006). Well-preserved shells appear more transparent and "glassy" whereas diagenetically altered shells appear more opaque and "frosty." Studies of shell microstructure and geochemistry of glassy and frosty foraminiferal shells have indicated that frosty

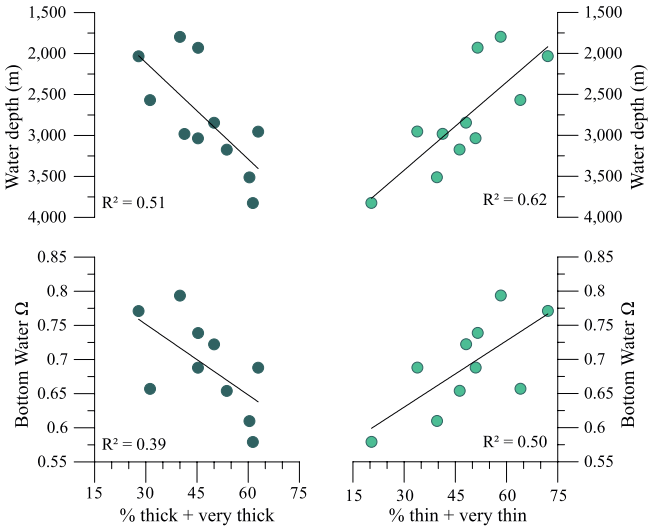

Figure 8. The total of thick and very thick shells relative to the total number of shells is moderately well correlated with core depth ($R^2 = 0.51$) and weakly correlated with bottom water saturation ($R^2 = 0.39$). The total of thin and very thin shells relative to the total number of measured shells (%wp) is well correlated with core depth ($R^2 = 0.62$) and moderately well correlated with bottom water calcite saturation ($R^2 = 0.50$).

shells have diagenetically altered shell walls and different isotopic, radioisotopic, and trace element compositions relative to glassy shells (Edgar et al., 2015; Gibson et al., 2016; Metcalfe, 2013; Pearson & Burgess, 2008; Sexton et al., 2006; Wycech et al., 2016). Our thin and very thin shells were predominantly glassy to partially glassy, whereas the thick and very thick shells were generally frosty.

Work here suggests that thin and very thin shells are indicative of generally well-preserved *G. bulloides* in a given sample, and thick and very thick shells are indicative of a more poorly preserved fraction. The proportion of well-preserved shells (thin + very thin shells) relative to the total shells (% well-preserved, %wp) is a way to quantify the shift in distribution of individual multicore core-tops and to apply a number to the visual shifts observed in the histograms. It can also be thought of as a way to quantify the proportion of "glassy" versus "frosty" individuals in a sample. The %wp calculation relies on the thin/thick threshold, which corresponds to the mean area density value of the total multicore core-top data and the max of the trap data. Because of this definition, the %wp corresponds to the percentage of shells that are better preserved than 50% of the core-top data and more poorly preserved than the "pristine" trap endmember.

The %wp (thin + very thin) from each of the Indian Ocean core-tops was well correlated with core depth ($R^2 = 0.62$) and moderately well correlated with bottom water carbonate saturation ($R^2 = 0.50$; Figure 8), suggesting that the proportion of well-preserved to poorly preserved shells in a sample provides a quantifiable measure of dissolution and diagenesis in marine sediment cores. Likewise, the proportion of poorly preserved shells (thick + very thick) was moderately well correlated with depth ($R^2 = 0.51$) and bottom water carbonate saturation ($R^2 = 0.39$; Figure 8). One can interpret a sample with a lower percentage of thin and very thin shells as having been exposed to waters that are more undersaturated with respect to carbonate ion resulting in dissolution and fragmentation of those shells. Likewise, a sample with a higher percentage of thin and very thin shells has not been sufficiently subjected to undersaturated waters to result in dissolution and fragmentation of those shells. With these bounds, the %wp metric has the potential as a non-destructive and analytically simple proxy for quantifying variability in the depth of the lysocline through time, whereas proxies for lysocline depth, such as $\%CaCO_3$, are often limited to suggesting only whether the core was generally below or above the CCD.

5. Core Top Area Density Calibrations

Our results indicate that sample preservation does impact individual *G. bulloides* area density values and the distribution of area density values in a sample, but this does not preclude the use of such samples for reconstructing surface ocean conditions. The core-top thin and very thin *G. bulloides* area densities have a similar relationship to surface ocean (CO_3^{2-}) as documented for *G. bulloides* in SBB sediment trap samples (Osborne et al., 2016, Figure 9). However, thick shells show a slight negative correlation with surface ocean (CO_3^{2-}) (Figure 9), inconsistent with results from culture, sediment trap, and plankton tow samples (Beer et al., 2010; Davis et al., 2017; Moy et al., 2009; Osborne et al., 2016; Weinkauf et al., 2016). An insufficient number of very thick shells precluded an assessment of the relationship of very thick shells with surface ocean (CO_3^{2-}). Our results suggest very thick shells are characteristic of diagenetic overprinting. Increased dissolution features in our SEM images suggest that thicker *G. bulloides* are not as well preserved (Figure 6). Partial dissolution and recrystallization or encrustation of foraminiferal calcite in deep corrosive waters can overprint the relationship of shell thickness to surface ocean conditions, accounting for the reversed trends in thick *G. bulloides*. The similar relationships between thin and very thin *G. bulloides* and surface ocean (CO_3^{2-}) in the Indian Ocean to those documented in the SBB sediment traps reinforces that grouping area density measurements into a narrow range of values can capture the influences related to genetic diversity

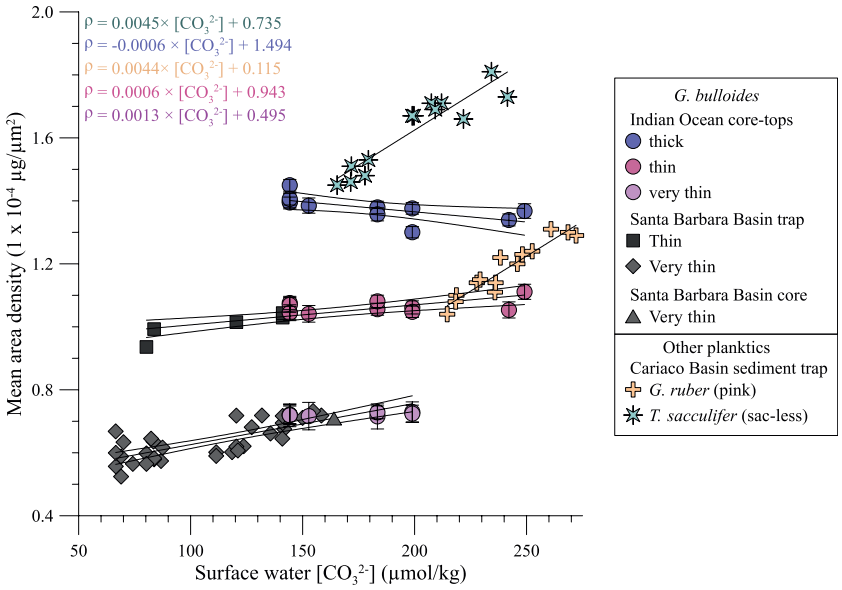

Figure 9. Area density carbonate ion calibrations for *G. bulloides* from Indian Ocean core tops and Santa Barbara Basin sediment trap (Osborne et al., 2016) and box core sediments from post-2000 CE (Osborne et al., 2020) compared with symbiont-bearing planktic foraminifera species *G. ruber* and *T. sacculifer* from the Cariaco Basin sediment trap (Marshall et al., 2013).

and shell preservation allowing the well-preserved (thin and very thin) shells to be used in reconstructing surface ocean conditions.

More generally, even very thin and thin *G. bulloides* appear less sensitive to shifts in surface ocean (CO_3^{2-}) than the planktic species, *G. ruber* and *T. sacculifer* (Henehan et al., 2017; Marshall et al., 2013; Figure 9). These species harbor photosynthetic algal symbionts that actively modify the chemistry by increasing the pH of the shell microenvironment during photosynthesis promoting daytime calcification (Jørgensen et al., 1985; Lombard et al., 2010; Rink et al., 1998; Wolf-Gladrow et al., 1999) and increasing calcification rates (Bé et al., 1982). The calcification rate observed for *G. bulloides* (0.3 ug/day) is one tenth to one third *G. ruber* (1 ug/day) and *T. sacculifer* (3 ug/day) (Allen et al., 2016). Although *G. bulloides* show a less sensitive relationship between area density with a given change in surface ocean carbonate ion concentration, the lack of symbionts provides a more straightforward relationship with carbonate chemistry that may be preferable for paleo-reconstructions.

Glacial-interglacial records of surface ocean (CO_3^{2-}) estimate an increase of ~60 µmol/kg over the last deglaciation (~18–11 ka ago), using boron isotopes and boron to calcium ratios (Foster, 2008; Yu et al., 2013). Our core-top area density calibration for (CO_3^{2-}) predicts that a ~60 µmol/kg increase would correspond to a 0.080×10^4 µg/µm^2 decrease in the area density value of very thin shells and a decrease of 0.045×10^4 µg/µm^2 for thin shells relative to Holocene values (Figure 9) highlighting the need to utilize shells minimally impacted by diagenesis. Consequently, %wp can be used to assess sediment core suitability for down-core area density surface ocean (CO_3^{2-}) reconstructions and to establish the usefulness of a given core or site for geochemical studies.

6. Conclusions

In this study we utilize a collection of Indian Ocean multicore core-tops to assess the influence of diagenesis on area density values. Although dissolution and preservation impact planktic area density values, we find that can we account for some of these influences and utilize them to provide information about past ocean chemistry. Our results suggest that grouping area density measurements in a narrow range can reveal influences related to cryptic speciation and shell preservation, up to a maximum area density value (~0.122×10^4 µg/µm^2) above which the surface ocean signature is no longer retained. Area density

values were classified as very thick (>0.160 × 10^4 μg/μm^2), thick (0.122 × 10^4–0.160 × 10^4 μg/μm^2), thin (0.087 × 10^4–0.122 × 10^4 μg/μm^2), and very thin (<0.087 × 10^4 μg/μm^2). Both thin and very thin shells appear to retain a surface ocean signature correlating with surface ocean carbonate ion concentrations. In contrast, thick *G. bulloides* shells show an opposite trend, which is likely a result of recrystallization or authigenic crust formation.

Analysis of the distribution of area density values provides a method for assessing sample preservation. We suggest dissolution and fragmentation decreases the number of very thin shells whereas recrystallization or formation of authigenic carbonate crusts results in an increased number of very thick shells. Accordingly, an increase in the proportion of very thick to very thin shells indicates reduced preservation. We have developed a metric; %wp, (percent well preserved) for assessing preservation by quantifying the distribution of well-preserved (thin and very thin) shells relative to the total measured shells in a sample. Our %wp metric has the potential for use as a proxy for deep ocean carbonate saturation and lysocline variability in addition to assessing the suitability of area density samples for surface ocean reconstructions.

Our results highlight the benefits of utilizing the distribution of area density values to reconstruct sedimentary preservation and deep ocean lysocline variability along with assessing the area density values of well-preserved shells (thin and very thin) to reconstruct surface ocean carbonate variability. This dual surface and deep ocean approach has the potential as a proxy for reconstructing oceanic carbon storage. The non-destructive nature of the area density proxy means that it can be used to evaluate foraminifera preservation before their use for geochemical analyses. Geochemical analyses can then be paired with area density estimates of surface ocean carbonate ion and deep ocean dissolution, all from the same individual foraminifera, making area density a powerful tool for enhancing our understanding of past ocean chemistry.

Conflict of Interest

The authors declare no conflicts of interest relevant to this study.

Data Availability Statement

The datasets generated during this study have been archived at World Data Service for Paleoclimatology: https://www.ncdc.noaa.gov/paleo/study/33332. Click or tap if you trust this link. https://www.ncdc.noaa.gov/paleo/study/33332.

Acknowledgments
This research was supported by the National Science Foundation (OCE 2002630 and OCE 1559080) and the Science Pathways Scholar Program at Barnard College. Much of this work was completed from the author's homes during the New York COVID Pause.

References

Allen, K. A., Hönisch, B., Eggins, S. M., Haynes, L. L., Rosenthal, Y., & Yu, J. (2016). Trace element proxies for surface ocean conditions: A synthesis of culture calibrations with planktic foraminifera. *Geochimica et Cosmochimica Acta*, *193*, 197–221. https://doi.org/10.1016/j.gca.2016.08.015

Barker, S., & Elderfield, H. (2002). Foraminiferal calcification response to glacial-interglacial changes in atmospheric CO2. *Science*, *297*(5582), 833–836. https://doi.org/10.1126/science.1072815

Bé, A. W. H. (1977). An ecological, zoogeographic and taxonomic review of recent planktonic foraminifera. In A. T. S. Ramsay (Ed.), *Oceanic micropaleontology* (pp. 1–100). New York: Academic Press.

Bé, A. W. H. (1980). Gametogenic calcification in a spinose planktonic foraminifer, Globigerinoides sacculifer (Brady). *Marine Micropaleontology*, *5*, 283–310. https://doi.org/10.1016/0377-8398(80)90014-6

Bé, A. W. H., Morse, J. W., & Harrison, S. M. (1975). Progressive dissolution and ultrastructural breakdown of planktonic foraminifera. In W. V. Sliter, A. W. H. Bé, & W. H. Berger (Eds.), *Dissolution of deep-sea carbonates* (pp. 27–55). Cushman Foundation for Foraminiferal Research.

Bé, A. W. H., Spero, H. J., & Anderson, O. R. (1982). Effects of symbiont elimination and reinfection on the life processes of the planktonic foraminifer Globigerinoides sacculifer. *Marine Biology*, *70*(1), 73–86. https://doi.org/10.1007/BF00397298

Bé, A. W. H., & Tolderlund, D. S. (1971). Distribution and ecology of living planktonic Foraminifera in surface waters of the Atlantic and Indian Oceans. In B. M. Funnel, & W. R. Reidel (Eds.), *Microplaeontology of oceans* (pp. 105–149). London: Cambridge University Press.

Beer, C. J., Schiebel, R., & Wilson, P. A. (2010). Testing planktic foraminiferal shell weight as a surface water [CO_3^{2-}] proxy using plankton net samples. *Geology*, *38*(2), 103–106. https://doi.org/10.1130/G30150.1

Berger, W. H. (1970). Planktonic Foraminifera: Selective solution and the lysocline. *Marine Geology*, *8*(2), 111–138. https://doi.org/10.1016/0025-3227(70)90001-0

Bijma, J., Hönisch, B., & Zeebe, R. E. (2002). Impact of the ocean carbonate chemistry on living foraminiferal shell weight: Comment on "Carbonate ion concentration in glacial-age deep waters of the Caribbean Sea" by W. S. Broecker and E. Clark: Comment. *Geochemistry, Geophysics, Geosystems*, *3*(11), 1–7. https://doi.org/10.1029/2002GC000388

Branson, O., Read, E., Redfern, S. A. T., Rau, C., & Elderfield, H. (2015). Revisiting diagenesis on the Ontong Java Plateau: Evidence for authigenic crust precipitation in *Globorotalia tumida*. *Paleoceanography*, *30*(11), 1490–1502. https://doi.org/10.1002/2014PA002759

Broecker, W., & Clark, E. (2001). An evaluation of Lohmann's foraminifera weight dissolution index. *Paleoceanography*, *16*(5), 531–534. https://doi.org/10.1029/2000PA000600

Brown, S. J., & Elderfield, H. (1996). Variations in Mg/Ca and Sr/Ca ratios of planktonic foraminifera caused by postdepositional dissolution: Evidence of shallow Mg-dependent dissolution. *Paleoceanography*, *11*(5), 543–551. https://doi.org/10.1029/96PA01491

Darling, K. F., Kucera, M., Wade, C. M., von Langen, P., & Pak, D. (2003). Seasonal distribution of genetic types of planktonic foraminifer morphospecies in the Santa Barbara Channel and its paleoceanographic implications. *Paleoceanography*, *18*(2), 1032. https://doi.org/10.1029/2001PA000723

Darling, K. F., & Wade, C. M. (2008). The genetic diversity of planktic foraminifera and the global distribution of ribosomal RNA genotypes. *Marine Micropaleontology*, *67*(3–4), 216–238. https://doi.org/10.1016/j.marmicro.2008.01.009

Darling, K. F., Wade, C. M., Siccha, M., Trommer, G., Schulz, H., Abdolalipour, S., & Kurasawa, A. (2017). Genetic diversity and ecology of the planktonic foraminifers Globigerina bulloides, Turborotalita quinqueloba and Neogloboquadrina pachyderma off the Oman margin during the late SW Monsoon. *Marine Micropaleontology*, *137*, 64–77. https://doi.org/10.1016/j.marmicro.2017.10.006

Darling, K. F., Wade, C. M., Stewart, I. A., Kroon, D., Dingle, R., & Brown, A. J. L. (2000). Molecular evidence for genetic mixing of Arctic and Antarctic subpolar populations of planktonic foraminifers. *Nature*, *405*(6782), 43–47. https://doi.org/10.1038/35011002

Davis, C. V., Rivest, E. B., Hill, T. M., Gaylord, B., Russell, A. D., & Sanford, E. (2017). Ocean acidification compromises a planktic calcifier with implications for global carbon cycling. *Scientific Reports*, *7*(1), 2225. https://doi.org/10.1038/s41598-017-01530-9

de Moel, H., Ganssen, G. M., Peeters, F. J. C., Jung, S. J. A., Kroon, D., Brummer, G. J. A., & Zeebe, R. E. (2009). Planktic foraminiferal shell thinning in the Arabian Sea due to anthropogenic ocean acidification? *Biogeosciences*, *6*(9), 1917–1925. https://doi.org/10.5194/bg-6-1917-2009

Detlef, H., Sosdian, S. M., Kender, S., Lear, C. H., & Hall, I. R. (2020). Multi-elemental composition of authigenic carbonates in benthic foraminifera from the eastern Bering Sea continental margin (international ocean discovery program site U1343). *Geochimica et Cosmochimica Acta*, *268*, 1–21. https://doi.org/10.1016/j.gca.2019.09.025

Dickson, A. G. (1990). Thermodynamics of the dissociation of boric acid in synthetic seawater from 273.15 to 318.15 K. *Deep Sea Research Part A. Oceanographic Research Papers*, *37*(5), 755–766. https://doi.org/10.1016/0198-0149(90)90004-F

Dickson, A. G., & Riley, J. P. (1979). The estimation of acid dissociation constants in seawater media from potentionmetric titrations with strong base. I. The ionic product of water — Kw. *Marine Chemistry*, *7*(2), 89–99. https://doi.org/10.1016/0304-4203(79)90001-X

Dittert, N., & Henrich, R. (2000). Carbonate dissolution in the South Atlantic Ocean: Evidence from ultrastructure breakdown in Globigerina bulloides. *Deep Sea Research Part I: Oceanographic Research Papers*, *47*(4), 603–620. https://doi.org/10.1016/S0967-0637(99)00069-2

Edgar, K. M., Anagnostou, E., Pearson, P. N., & Foster, G. L. (2015). Assessing the impact of diagenesis on $\delta^{11}B$, $\delta^{13}C$, $\delta^{18}O$, Sr/Ca, and B/Ca values in fossil planktic foraminiferal calcite. *Geochimica et Cosmochimica Acta*, *166*, 189–209. https://doi.org/10.1016/j.gca.2015.06.018

Field, D. B. (2004). Variability in vertical distributions of planktonic foraminifera in the California Current: Relationships to vertical ocean structure. *Paleoceanography*, *19*(2), PA2014. https://doi.org/10.1029/2003PA000970

Foster, G. L. (2008). Seawater pH, pCO2 and [CO2−3] variations in the Caribbean Sea over the last 130 kyr: A boron isotope and B/Ca study of planktic foraminifera. *Earth and Planetary Science Letters*, *271*(1–4), 254–266. https://doi.org/10.1016/j.epsl.2008.04.015

Gibson, K. A., Thunell, R. C., Machain-Castillo, M. L., Fehrenbacher, J., Spero, H. J., Wejnert, K., et al. (2016). Evaluating controls on planktonic foraminiferal geochemistry in the Eastern Tropical North Pacific. *Earth and Planetary Science Letters*, *452*, 90–103. https://doi.org/10.1016/j.epsl.2016.07.039

Hamilton, C. P., Spero, H. J., Bijma, J., & Lea, D. W. (2008). Geochemical investigation of gametogenic calcite addition in the planktonic foraminifera *Orbulina universa*. *Marine Micropaleontology*, *68*(3–4), 256–267. https://doi.org/10.1016/j.marmicro.2008.04.003

Hemleben, C., Spindler, M., & Anderson, O. R. (1989). *Modern planktonic foraminifera*. New York, NY: Springer-Verlag. https://doi.org/10.1007/978-1-4612-3544-6

Henehan, M. J., Evans, D., Shankle, M., Burke, J. E., Foster, G. L., Anagnostou, E., et al. (2017). Size-dependent response of foraminiferal calcification to seawater carbonate chemistry. *Biogeosciences*, *14*(13), 3287–3308. https://doi.org/10.5194/bg-14-3287-2017

IPCC. (2014). *Climate change 2014: Synthesis report.* (Contribution of working groups I, II and III to the fifth assessment report of the intergovernmental panel on climate change) (p. 151). Geneva, Switzerland: Intergovernmental Panel on Climate Change.

Iwasaki, S., Kimoto, K., Kuroyanagi, A., & Kawahata, H. (2017). Horizontal and vertical distributions of planktic foraminifera in the subarctic Pacific. *Marine Micropaleontology*, *130*, 1–14. https://doi.org/10.1016/j.marmicro.2016.12.001

Jørgensen, B. B., Erez, J., Revsbech, P., & Cohen, Y. (1985). Symbiotic photosynthesis in a planktonic foraminiferan, Globigerinoides sacculifer (Brady), studied with microelectrodes1. *Limnology and Oceanography*, *30*(6), 1253–1267. https://doi.org/10.4319/lo.1985.30.6.1253

Kretschmer, K., Jonkers, L., Kucera, M., & Schulz, M. (2018). Modeling seasonal and vertical habitats of planktonic foraminifera on a global scale. *Biogeosciences*, *15*(14), 4405–4429. https://doi.org/10.5194/bg-15-4405-2018

Kuroyanagi, A., & Kawahata, H. (2004). Vertical distribution of living planktonic foraminifera in the seas around Japan. *Marine Micropaleontology*, *53*(1–2), 173–196. https://doi.org/10.1016/j.marmicro.2004.06.001

Lavigne, H., Epitalon, J.-M., & Gattuso, J.-P. (2011). *Seacarb: Seawater carbonate chemistry with R*. [R package version 3.0]. Retrieved from http://CRAN.R-project.org/package=seacarb

Lohmann, G. P. (1995). A model for variation in the chemistry of planktonic foraminifera due to secondary calcification and selective dissolution. *Paleoceanography*, *10*(3), 445–457. https://doi.org/10.1029/95PA00059

Lombard, F., da Rocha, R. E., Bijma, J., & Gattuso, J.-P. (2010). Effect of carbonate ion concentration and irradiance on calcification in planktonic foraminifera. *Biogeosciences*, *7*(1), 247–255. https://doi.org/10.5194/bg-7-247-2010

Lorens, R. B., Williams, D. F., & Bender, M. L. (1977). The early nonstructural chemical diagenesis of foraminiferal calcite. *SEPM Journal of Sedimentary Research*, *47*, 1602–1609. https://doi.org/10.1306/212F73C9-2B24-11D7-8648000102C1865D

Lueker, T. J., Dickson, A. G., & Keeling, C. D. (2000). Ocean pCO2 calculated from dissolved inorganic carbon, alkalinity, and equations for K1 and K2: Validation based on laboratory measurements of CO2 in gas and seawater at equilibrium. *Marine Chemistry*, *70*(1–3), 105–119. https://doi.org/10.1016/S0304-4203(00)00022-0

Marshall, B. J., Thunell, R. C., Henehan, M. J., Astor, Y., & Wejnert, K. E. (2013). Planktonic foraminiferal area density as a proxy for carbonate ion concentration: A calibration study using the Cariaco Basin ocean time series. *Paleoceanography*, *28*(2), 363–376. https://doi.org/10.1002/palo.20034

Marshall, B. J., Thunell, R. C., Spero, H. J., Henehan, M. J., Lorenzoni, L., & Astor, Y. (2015). Morphometric and stable isotopic differentiation of Orbulina universa morphotypes from the Cariaco Basin, Venezuela. *Marine Micropaleontology*, *120*, 46–64. https://doi.org/10.1016/j.marmicro.2015.08.001

Metcalfe, B. (2013, December 17). *Planktonic foraminifera: From production to preservation of the oceanographic signal*. Amsterdam, Netherlands: Vrije Universiteit Amsterdam.

Millo, C., Sarnthein, M., Erlenkeuser, H., Grootes, P. M., & Andersen, N. (2005). Methane-induced early diagenesis of foraminiferal tests in the southwestern Greenland Sea. *Marine Micropaleontology*, *58*(1), 1–12. https://doi.org/10.1016/j.marmicro.2005.07.003

Morard, R., Quillévéré, F., Escarguel, G., de Garidel-Thoron, T., de Vargas, C., & Kucera, M. (2013). Ecological modeling of the temperature dependence of cryptic species of planktonic foraminifera in the Southern Hemisphere. *Palaeogeography, Palaeoclimatology, Palaeoecology*, *391*, 13–33. https://doi.org/10.1016/j.palaeo.2013.05.011

Mortyn, P. G., & Charles, C. D. (2003). Planktonic foraminiferal depth habitat and $\delta^{18}O$ calibrations: Plankton tow results from the Atlantic sector of the Southern Ocean. *Paleoceanography*, *18*(2), 1037. https://doi.org/10.1029/2001PA000637

Moy, A. D., Howard, W. R., Bray, S. G., & Trull, T. W. (2009). Reduced calcification in modern Southern Ocean planktonic foraminifera. *Nature Geoscience*, *2*(4), 276–280. https://doi.org/10.1038/ngeo460

Ortiz, J. D., Mix, A. C., & Collier, R. W. (1995). Environmental control of living symbiotic and asymbiotic foraminifera of the California Current. *Paleoceanography*, *10*(6), 987–1009. https://doi.org/10.1029/95PA02088

Osborne, E. B., Thunell, R. C., Gruber, N., Feely, R. A., & Benitez-Nelson, C. R. (2020). Decadal variability in twentieth-century ocean acidification in the California Current ecosystem. *Nature Geoscience*, *13*(1), 43–49. https://doi.org/10.1038/s41561-019-0499-z

Osborne, E. B., Thunell, R. C., Marshall, B. J., Holm, J. A., Tappa, E. J., Benitez-Nelson, C., et al. (2016). Calcification of the planktonic foraminifera *Globigerina bulloides* and carbonate ion concentration: Results from the Santa Barbara Basin. *Paleoceanography*, *31*(8), 1083–1102. https://doi.org/10.1002/2016PA002933

Pearson, P. N., & Burgess, C. E. (2008). Foraminifer test preservation and diagenesis: Comparison of high latitude Eocene sites. *Geological Society, London, Special Publications*, *303*(1), 59–72. https://doi.org/10.1144/SP303.5

Pearson, P. N., Ditchfield, P. W., Singano, J., Harcourt-Brown, K. G., Nicholas, C. J., Olsson, R. K., et al. (2001). Warm tropical sea surface temperatures in the Late Cretaceous and Eocene epochs. *Nature*, *413*(6855), 481–487. https://doi.org/10.1038/35097000

Peeters, F. J. C., & Brummer, G.-J. A. (2002). The seasonal and vertical distribution of living planktic foraminifera in the NW Arabian Sea. *Geological Society, London, Special Publications*, *195*, 463–497. https://doi.org/10.1144/GSL.SP.2002.195.01.26

Pena, L. D., Calvo, E., Cacho, I., Eggins, S., & Pelejero, C. (2005). Identification and removal of Mn-Mg-rich contaminant phases on foraminiferal tests: Implications for Mg/Ca past temperature reconstructions: Mg/Ca. *Geochemistry, Geophysics, Geosystems*, *6*(9), Q09P02. https://doi.org/10.1029/2005GC000930

Perez, F. F., & Fraga, F. (1987). Association constant of fluoride and hydrogen ions in seawater. *Marine Chemistry*, *21*(2), 161–168. https://doi.org/10.1016/0304-4203(87)90036-3

Peterson, L. C., & Prell, W. L. (1985). Carbonate dissolution in recent sediments of the eastern equatorial Indian Ocean: Preservation patterns and carbonate loss above the lysocline. *Marine Geology*, *64*(3–4), 259–290. https://doi.org/10.1016/0025-3227(85)90108-2

Qin, B., Li, T., Xiong, Z., Algeo, T. J., & Chang, F. (2017). Deepwater carbonate ion concentrations in the western tropical Pacific since 250 ka: Evidence for oceanic carbon storage and global climate influence. *Paleoceanography*, *32*(4), 351–370. https://doi.org/10.1002/2016PA003039

Regenberg, M., Regenberg, A., Garbe-Schönberg, D., & Lea, D. W. (2014). Global dissolution effects on planktonic foraminiferal Mg/Ca ratios controlled by the calcite-saturation state of bottom waters. *Paleoceanography*, *29*(3), 127–142. https://doi.org/10.1002/2013PA002492

Reimers, C. E., Ruttenberg, K. C., Canfield, D. E., Christiansen, M. B., & Martin, J. B. (1996). Porewater pH and authigenic phases formed in the uppermost sediments of the Santa Barbara Basin. *Geochimica et Cosmochimica Acta*, *60*(21), 4037–4057. https://doi.org/10.1016/S0016-7037(96)00231-1

Reynolds, L., & Thunell, R. C. (1985). Seasonal succession of planktonic foraminifera in the subpolar North Pacific. *The Journal of Foraminiferal Research*, *15*(4), 282–301. https://doi.org/10.2113/gsjfr.15.4.282

Rink, S., Kühl, M., Bijma, J., & Spero, H. J. (1998). Microsensor studies of photosynthesis and respiration in the symbiotic foraminifer Orbulina universa. *Marine Biology*, *131*(4), 583–595. https://doi.org/10.1007/s002270050350

Sadekov, A. Y., Darling, K. F., Ishimura, T., Wade, C. M., Kimoto, K., Singh, A. D., et al. (2016). Geochemical imprints of genotypic variants of *Globigerina bulloides* in the Arabian Sea: Geochemistry of Genotypic Variants. *Paleoceanography*, *31*(10), 1440–1452. https://doi.org/10.1002/2016PA002947

Sautter, L. R., & Thunell, R. C. (1989). Seasonal succession of planktonic foraminifera; results from a four-year time-series sediment trap experiment in the Northeast Pacific. *Journal of Foraminiferal Research*, *19*(4), 253–267. https://doi.org/10.2113/gsjfr.19.4.253

Sautter, L. R., & Thunell, R. C. (1991). Planktonic foraminiferal response to upwelling and seasonal hydrographic conditions; sediment trap results from San Pedro Basin, Southern California Bight. *Journal of Foraminiferal Research*, *21*(4), 347–363. https://doi.org/10.2113/gsjfr.21.4.347

Savin, S. M., & Douglas, R. G. (1973). Stable isotope and magnesium geochemistry of recent planktonic foraminifera from the South Pacific. *Geological Society of America Bulletin*, *84*(7), 2327–2342. https://doi.org/10.1130/0016-7606(1973)84<2327:SIAMGO>2.0.CO;2

Schiebel, R., Barker, S., Lendt, R., Thomas, H., & Bollmann, J. (2007). Planktic foraminiferal dissolution in the twilight zone. *Deep Sea Research Part II: Topical Studies in Oceanography*, *54*(5–7), 676–686. https://doi.org/10.1016/j.dsr2.2007.01.009

Schiebel, R., Bijma, J., & Hemleben, C. (1997). Population dynamics of the planktic foraminifer Globigerina bulloides from the eastern North Atlantic. *Deep Sea Research Part I: Oceanographic Research Papers*, *44*(9), 1701–1713. https://doi.org/10.1016/S0967-0637(97)00036-8

Schindelin, J., Arganda-Carreras, I., Frise, E., Kaynig, V., Longair, M., Pietzsch, T., et al. (2012). Fiji: An open-source platform for biological-image analysis. *Nature Methods*, *9*(7), 676–682. https://doi.org/10.1038/nmeth.2019

Sexton, P. F., Wilson, P. A., & Pearson, P. N. (2006). Microstructural and geochemical perspectives on planktic foraminiferal preservation: "Glassy" versus "Frosty. *Geochemistry, Geophysics, Geosystems*, *7*(12), Q12P19. https://doi.org/10.1029/2006GC001291

Spero, H. J., & Lea, D. W. (1996). Experimental determination of stable isotope variability in Globigerina bulloides: Implications for paleoceanographic reconstructions. *Marine Micropaleontology*, *28*(3–4), 231–246. https://doi.org/10.1016/0377-8398(96)00003-5

Thunell, R. C., & Reynolds, L. A. (1984). Sedimentation of planktonic foraminifera: Seasonal changes in species flux in the panama basin. *Micropaleontology*, *30*(3), 243. https://doi.org/10.2307/1485688

Waters, J., Millero, F. J., & Woosley, R. J. (2014). Corrigendum to "The free proton concentration scale for seawater pH", [MARCHE: 149 (2013) 8–22]. *Marine Chemistry*, *165*, 66–67. https://doi.org/10.1016/j.marchem.2014.07.004

Weinkauf, M. F. G., Kunze, J. G., Waniek, J. J., & Kučera, M. (2016). Seasonal variation in shell calcification of planktonic foraminifera in the NE atlantic reveals species-specific response to temperature, productivity, and optimum growth conditions. *PloS One*, *11*(2), e0148363. https://doi.org/10.1371/journal.pone.0148363

Wilke, I., Meggers, H., & Bickert, T. (2009). Depth habitats and seasonal distributions of recent planktic foraminifers in the Canary Islands region (29°N) based on oxygen isotopes. *Deep Sea Research Part I: Oceanographic Research Papers*, *56*(1), 89–106. https://doi.org/10.1016/j.dsr.2008.08.001

Wolf-Gladrow, D. A., Bijma, J., & Zeebe, R. E. (1999). Model simulation of the carbonate chemistry in the microenvironment of symbiont bearing foraminifera. *Marine Chemistry*, *64*(3), 181–198. https://doi.org/10.1016/S0304-4203(98)00074-7

Wycech, J., Kelly, D. C., & Marcott, S. (2016). Effects of seafloor diagenesis on planktic foraminiferal radiocarbon ages. *Geology*, *44*(7), 551–554. https://doi.org/10.1130/G37864.1

Yu, J., Thornalley, D. J. R., Rae, J. W. B., & McCave, N. I. (2013). Calibration and application of B/Ca, Cd/Ca, and $\delta^{11}B$ in *Neogloboquadrina pachyderma* (sinistral) to constrain CO_2 uptake in the subpolar North Atlantic during the last deglaciation. *Paleoceanography*, *28*(2), 237–252. https://doi.org/10.1002/palo.20024